1

INTRODUCTION

P. Pramanick and P. Bhartia

The history of the development of microwave circuits has in many ways followed that of the lower frequency electronics circuits. There have been constant pressures in both these disciplines to move from tubes to solid state devices and from large components to small and to the development of integrated circuits, devices, and systems. However, unlike the electronics field, where a large public impact was possible and strong consumer demand generated through ownership of radios, digital watches, calculators, television sets, video cassette recorders, and so on, the microwave oven seems to be the single piece of equipment that comes to the layman's mind when the word *microwaves* is mentioned. The greatest impact and perhaps use of microwave circuits and systems has been in areas such as communications, radar, electronic warfare, navigation, surveillance, and weapon guidance systems, which are largely military in nature and have been supported strongly by the defense community. Although there is also a lucrative market for defense-products-oriented industries, the profits are often limited by small-volume, limited customers due to export restrictions, and hence the drive for development in the area of microwave circuits seems traditionally to have lagged behind that of electronic circuits. For example, electronic integrated circuits (ICs) on chips were available commercially long before microwave integrated circuits (MICs) were.

The current trend in microwave technology is toward circuit miniaturization, high-level integration, improved reliability, low power consumption, cost reduction, and high-volume applications. Component size and performance are prime factors in the design of electronic systems for satellite communications, phased-array radar systems, electronic warfare, and other military applica-

Microwave Solid State Circuit Design, 2nd Edition, Edited by Inder Bahl and Prakash Bhartia
ISBN 0-471-20755-1

tions, while small size and low cost drive the consumer electronics market. Monolithic microwave integrated circuits (MMICs) based on gallium arsenide (GaAs) technology are the key to meeting the above requirements. They play an increasing role in consumer electronics dealing with information transfer, communications, automotive applications, and entertainment. With MMIC technology a typical microwave subsystem can be produced on a single chip at costs of less than $100 while simpler single-function chips cost less than $10. Some very simple function chips are now produced at costs as low as $1. While most MMICs currently in production operate in the 0.5- to 30-GHz microwave range, there are increasing applications in the millimeter-wave (mmW) spectrum (30–300 GHz) as higher frequency transistors mature. Monolithic technology is particularly beneficial to mmW applications through the elimination of the parasitic effects of bond wires that connect discrete components in conventional hybrid structures.

1.1 CHARACTERISTICS OF MICROWAVES/MILLIMETER WAVES

The term *microwave/millimeter wave* generally refers to the frequency range where wavelengths are of the order of centimeters down to 1 mm. Some authors have suggested that microwave/millimeter-wave spectrum corresponds to the frequency range 1–300 GHz (wavelength 30 cm–1 mm), but the generally accepted convention is that the frequency range 300 MHz–300 GHz (wavelength 100 cm–1 mm) is more appropriate. Figure 1.1 depicts the position of the microwave and millimeter-wave part of the spectrum in relation to the rest of the electromagnetic spectrum.

In the microwave/millimeter-wave region, for convenience, a letter band designation has also been used to indicate the portion of the spectrum being referred to. Over the years, the radar community, for example, has created its own band designations, leading to general confusion. For example, *K*-band designates the frequency ranges 18–26.5 GHz, 19–27 GHz, 10.9–36 GHz, and 20–40 GHz in the radar users terminology, the U.K. frequency designation, the old U.S. military, and the new U.S. military designations, respectively. For the sake of clarity and uniformity, only the new U.S. military designation should be used. Figure 1.2 depicts the frequency band breakdown for the microwave/millimeter-wave region of interest for the purposes of this test.

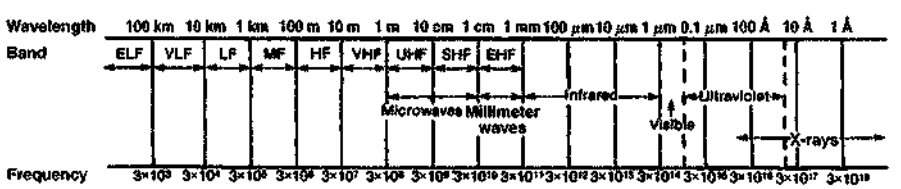

Figure 1.1 Electromagnetic spectrum.

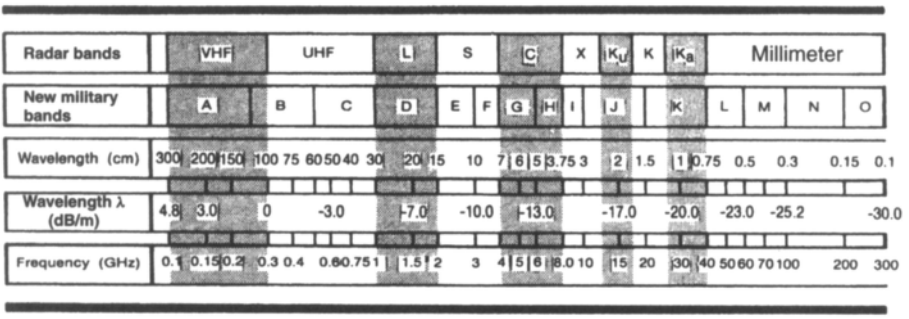

Figure 1.2 Band designation chart.

Some other features of microwave/millimeter waves are worth noting; for example, the decrease in wavelength as frequency increases corresponds to a reduction in component size, resulting in more compact systems and narrow beamwidths, which allow, for example, for greater resolution and precision in target tracking. Many advantages and disadvantages of microwave via-à-vis millimeter wave are discussed in Bhartia and Bahl [1].

Another interesting and important characteristic is the free-space propagation attenuation over the frequency range. As shown in Fig. 1.3, atmospheric absorption increases with frequency, but in addition, there exist high absorption windows in the millimeter-wave band due to atmospheric water vapor and oxygen. While this characteristic is not of significant interest for the purposes of

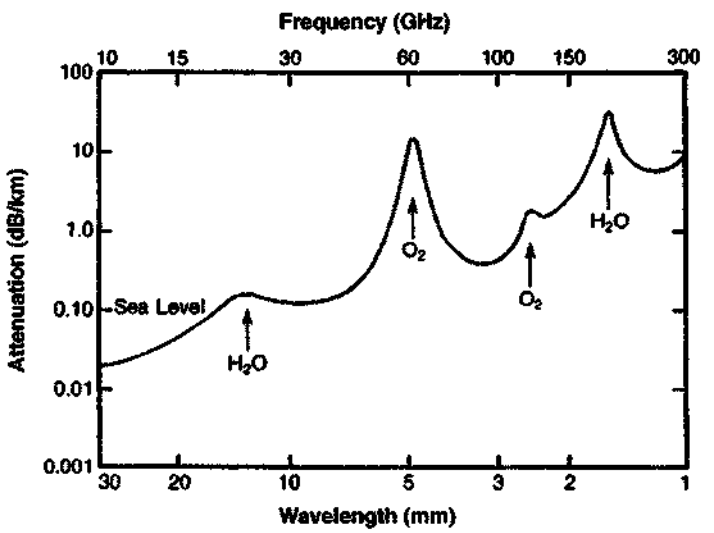

Figure 1.3 Atmospheric absorption as function of frequency.

this book in microwave circuits, it should be realized that a similar behavior occurs with transmission media, and one must choose the appropriate low-loss media for the frequency of operation of one's circuit.

1.2 HISTORY OF MICROWAVE PLANAR CIRCUITS

The first evolution of the conventional waveguide and coaxial line was a flat-strip coaxial transmission line used by Rumsey and Jamieson—as mentioned, for example, by Barrett [2] for producing an antenna system and power division network during World War II. This was gradually integrated with printed-circuit technology to result in the "microwave printed circuit" (MPC) reported by Barrett and Barnes [3] and soon developed into a printed-circuit waveguide handbook [4]. Shortly after Barrett and Barnes's [3] report on MPCs, the Federal Communications Research Laboratories announced the microstrip [5] and King [6] reported the "dielectric image line." The MPC concept was used in fabricating many components, such as directional couplers, filters, attenuators, and antennas. The microstrip is fundamental to IC design and is today being used extensively in its many forms in a large variety of circuits. Finally, the image line is an excellent transmission medium, particularly for millimeter-wave circuits.

Following the preceding developments, the MIC area grew rapidly in the 1960s. Between 1964 and 1968, the largest quantity production for a MIC was perhaps the 600 transmit/receive (T/R) modules produced by Texas Instruments for the molecular electronics for radar application (MERA) radar [7]. Many other significant developments also occurred over the 1960–1980 period, and it was evident that the field of MICs was fast maturing. Over these years, the idea of MMICs also evolved, where all microwave functions of analog circuits, as well as new digital applications, could be incorporated on a single chip [8]. In the earlier MICs and MMICs, high-resistivity *p*-type (boron) silicon was used as the microwave substrate and host for the devices. However, two factors have been primarily responsible for the emergence of GaAs in the development of MMICs. First, the semi-insulating substrate is almost an ideal dielectric medium for microstrip transmission; second is the GaAs field-effect transistor (FET), which is the workhorse of all analog ICs. The latter has benefited from the application of silicon processing technology. Thus, GaAs technology promises a new breed of components that will allow designers greater flexibility and lower cost approaches to achieve their design goals.

1.3 APPLICATIONS OF MICROWAVE PLANAR CIRCUITS

Microwave planar circuits can be applied to and substituted for the conventional form of microwave circuitry in virtually every application in the fields of communications, electronic warfare, radar, and weapon systems. In general,

the limitations are few, one fundamental one being the power-handling capability. However, realization of good matching circuitry has allowed high power levels to be achieved in some laboratory MMICs, but to achieve high powers while maintaining high yield still requires hybrid MIC as well as conventional waveguide and coaxial-line techniques. In many cases, requiring high power, such as space-based radar and the use of thousands of solid-state transmitter-receivers for an active aperture phased array, allows for power distribution and hence use of MMICs or MICs. Hopefully, the extensive number of T/R modules required will allow for a substantial cost reduction for MMICs over hybrid MICs or conventional circuitry.

Another area that should see high microwave planar circuit usage is electronic warfare. In particular, expendable systems such as expendable jammers and smart munitions using microwave/millimeter-wave guidance systems, both passive radiometer type and active radar, should benefit from the cost reductions and lower weight properties of these circuits. Naturally, satellite systems, where weight is an all-important issue due to high cost per kilogram of launched payload, also stand to benefit significantly from the use of this technology.

Similarly, receivers and transmitters for communications, electronic support measures, electronic countermeasures, and systems for electronic communication or signal intelligence (ELINT, COMINT, SIGINT) all make extensive use of microwave/millimeter-wave circuits and devices. As systems become more complex due to the nature of the electronic threat, hardware complexity increases, resulting in larger and heavier systems. Use of planar technology, and in particular MMICs, helps to achieve significant reduction in both these factors, thus making it possible to deploy these systems easily on aircraft, where space and power are driving constraints.

Most radars being built currently use hybrid circuitry that needs tweaking for optimum performance. In these cases, microwave planar circuits offer the advantages of smaller size, lighter weight, potentially lower cost, high reliability, broad-bandwidth capability, and function reproducibility. These advantages allow the development of active element phased radars with significant beam agility, multifunction capability, and reliability. In addition, in most applications the redundancy of the T/R modules that can be built in allows for the desirable feature of graceful degradation in case of failure. A typical active element configuration for one of these is shown in Fig. 1.4.

While the military and space applications stand to gain the most from use of planar microwave/millimeter-wave circuits, other unconventional applications, such as highway-traffic control using microwave systems and microwave sensor systems used in microwave heating and drying, will likewise see cost reductions and smaller sizes with the availability of multifunction monolithic circuits.

The advances in microwave/millimeter-wave planar circuits coupled with advances that are currently occurring in electro-optics, magneto-optics, microwave optics, and microwave acoustics point to exciting decades ahead for engineering and the sciences. In particular, these fields will have strong impact

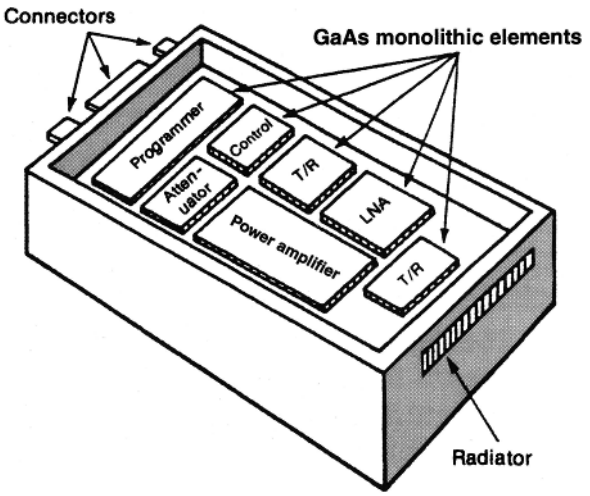

Figure 1.4 A T/R module using GaAs MMIC chips.

on consumer electronics and gadgets, while at the same time contributing in a large way to fields such as robotics, smart weapons, satellite technology and capabilities, smart-skins for aircraft, photonics, and smart built-in testing. Toward this objective, this text should serve as a reference for the fundamental microwave/millimeter-wave planar circuit active and passive components.

To make the book self-contained, in the next section, we discuss some fundamental concepts of microwave network theory and matrices of importance for circuit analysis and design.

1.4 MICROWAVE NETWORK THEORY

Microwave passive and active networks can be classified as multiport networks. Such networks are also known as N-port networks. Assuming the input and the output ports of an N-port microwave network are known, its frequency- and time-domain responses to a known excitation can be determined. For instance, if one of the ports of a transistor is terminated in a short circuit, the frequency response of the remaining two-port network can be obtained from the knowledge of the original three-port network. Also, in any microwave circuit, system or subsystem, there are many components connected in a certain fashion. The frequency response of this system can be obtained from knowledge of the individual components.

There are many equivalent ways in which the frequency response of a linear microwave network can be calculated [9]. This chapter deals with the representation of linear microwave networks as multiport black boxes.

1.4.1 Concepts of Equivalent Voltage and Current

The determination of network characteristics at microwave frequencies involves concepts that are substantially different from those used for low-frequency radio-frequency (RF) circuits for which voltages and currents, which determine impedance, can be uniquely defined. At microwave frequencies, use of neither high-frequency probes nor low-impedance current measurements are possible, because parasitic impedance and capacitance cannot be made small enough. In addition, the physical dimensions of a microwave circuit are no longer small compared to wavelength. Therefore, in most cases, the concepts of equivalent voltage and current are used. The equivalent voltage and current are so chosen that power transmitted along a transmission line is computed correctly using the equation

$$P = \tfrac{1}{2}\,\mathrm{Re}\int_S (E \times H)\,ds = \tfrac{1}{2}\,\mathrm{Re}(VI^*) \tag{1.1}$$

where '*' denotes the complex conjugate, and the power P is assumed to be flowing in the z direction; V and I are the equivalent voltage and current, respectively; E and H are the electric and magnetic fields, respectively, in the xy plane; and S is the cross-sectional area of the transmission line.

We can use the familiar definitions of voltage and current only in electrostatics. As soon as the electric field becomes time dependent, it generates a time-varying magnetic field, which in turn gives rise to a dynamic electric field. The electric voltage corresponding to this new dynamic electric field depends on the path of the line integral chosen to calculate the voltage.

Let us consider the transverse part of the electromagnetic (EM) field in a transmission line, for example, a coaxial line or a waveguide,

$$E_T^+ = \xi e_T(x, y)e^{-j\beta z} \tag{1.2a}$$

$$H_T^+ = \xi h_T(x, y)e^{-j\beta z} \tag{1.2b}$$

where ξ is a constant of proportionality, $e_T(x, y)$ and $h_T(x, y)$ are the normalized modal functions such that

$$\int_S [e_T(x, y) \times h_T(x, y)]\,ds = 1 \tag{1.2c}$$

and β is the propagation constant in the z direction.

According to Collin [9], the above fields are proportional to the equivalent voltage and current. Therefore,

$$E_T^+ = K_V V^+ e_T(x, y)e^{-j\beta z} \tag{1.3a}$$

$$H_T^+ = K_I I^+ h_T(x, y)e^{-j\beta z} \tag{1.3b}$$

where K_V is a constant of proportionality and V^+ and I^+ are the forward-going equivalent voltage and current, respectively. The transmitted power associated with the forward wave is given by

$$P^+ = \tfrac{1}{2}\,\mathrm{Re}\int_S (E_T^+ \times H_T^+)\,ds \tag{1.4}$$

Combining Eqs. (1.2c), (1.3a), (1.3b), and (1.4) gives

$$P^+ = \tfrac{1}{2}K_V K_I\,\mathrm{Re}(V^+ I^{+*}) \tag{1.5}$$

Comparing Eqs. (1.1) and (1.5) gives

$$K_V K_I = 1 \tag{1.6}$$

Using transmission line theory, we can write

$$\frac{V^+}{I^+} = Z_0 \tag{1.7}$$

where Z_0 is the characteristic impedance of the line. Comparing (1.2), (1.3), and (1.7), we get

$$\frac{K_I}{K_V} = Z_0 \tag{1.8}$$

Solving Eqs. (1.6) and (1.8) gives

$$K_V = \frac{1}{\sqrt{Z_0}} \tag{1.9a}$$

$$K_I = \sqrt{Z_0} \tag{1.9b}$$

The characteristic impedance Z_0 of a coaxial or two-conductor transmission line can be uniquely defined for the fundamental transverse-electromagnetic (TEM) mode. Therefore, the equivalent forward voltage and current can be uniquely expressed using Eqs. (1.2), (1.3), and (1.9) as

$$V^+ = \varsigma\sqrt{Z_0} \tag{1.10a}$$

$$I^+ = \frac{\varsigma}{\sqrt{Z_0}} \tag{1.10b}$$

Similarly, the backward voltage and current can be written as

$$V^- = \kappa\sqrt{Z_0} \tag{1.11a}$$

$$I^- = \frac{\kappa}{\sqrt{Z_0}} \tag{1.11b}$$

In Eqs. (1.10) and (1.11) ς and κ are proportionality constants.

If the transmission line supports a non-TEM mode, that is, transverse-electric (TE) or transverse-magnetic (TM) mode in a waveguide, the definition of the characteristic impedance cannot be unique. For example, if one considers the ratio of the fundamental mode average power flowing through a rectangular waveguide and the voltage at the center of the broad wall, the characteristic impedance assumes the form

$$Z_0(f) = \frac{2b}{a}\frac{\eta_0}{\sqrt{1-(f_c/f)^2}} \tag{1.12a}$$

where a and b are the width and the height of the waveguide cross section, respectively; η_0 is the free-space impedance; f is the operating frequency; and f_c is the cutoff frequency of the fundamental mode.

If one considers the ratio of the same voltage and the total longitudinal current, then the characteristic impedance assumes the form

$$Z_0(f) = \left(\frac{\pi b}{2a}\right)\frac{\eta_0}{\sqrt{1-(f_c/f)^2}} \tag{1.12b}$$

Also, if one considers the ratio of the fundamental mode average longitudinal power and the total longitudinal current, one gets

$$Z_0(f) = \left(\frac{\pi^2 b}{8a}\right)\frac{\eta_0}{\sqrt{1-(f_c/f)^2}} \tag{1.12c}$$

Therefore, unique definitions for equivalent voltage and current are not possible.

1.4.2 Admittance and Impedance Matrices

Consider Fig. 1.5. The accessible ports are denoted by $1, 2, 3, \ldots, N$. In addition, there is a ground terminal at each port. Let us assume that the I_i $(i = 1, 2, 3, \ldots, N)$ denote the port currents and the V_i $(i = 1, 2, 3, \ldots, N)$ denote the port voltages, respectively, at ports 1–N. The admittance matrix of the network is defined as

$$[I] = [Y][V] \tag{1.13}$$

where

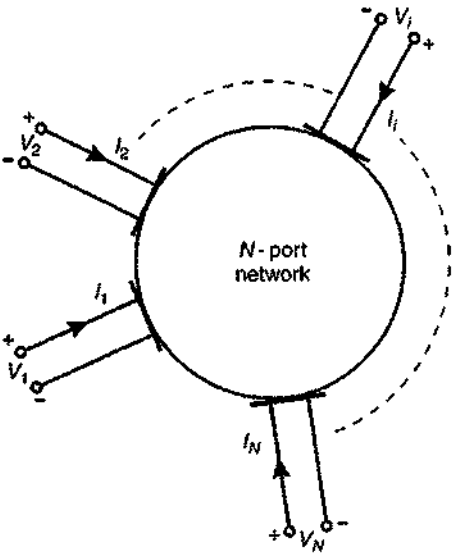

Figure 1.5 Schematic of N-port network.

$$[I] = \begin{bmatrix} I_1 \\ I_2 \\ \vdots \\ I_N \end{bmatrix} \qquad [V] = \begin{bmatrix} V_1 \\ V_2 \\ \vdots \\ V_N \end{bmatrix} \qquad [Y] = \begin{bmatrix} Y_{11} & Y_{12} & \cdots & Y_{1N} \\ Y_{21} & Y_{22} & \cdots & Y_{2N} \\ \vdots & \vdots & \ddots & \vdots \\ Y_{N1} & Y_{N2} & \cdots & Y_{NN} \end{bmatrix} \tag{1.14}$$

The admittance matrix $[Y]$ is obtained by nodal analysis of the network and then solving for the port currents or voltages. The corresponding impedance matrix is defined as

$$[Z] = [Y]^{-1} \tag{1.15}$$

The above admittance and impedance matrices are also known as unnormalized admittance and impedance matrices, respectively.

A microwave component or a subsystem is connected to a larger system. As a result, each port of a component is terminated by an impedance offered by the larger system to which it is connected. Let us assume that the impedance vector gives the set of terminating impedances offered by the embedding system

$$[Z_I] = [Z_{I1} \quad Z_{I2} \quad \cdots \quad Z_{IN}] \tag{1.16}$$

We define a new set of port voltages and currents, known as the normalized port voltages and currents, as

$$v_i = \frac{V_i}{\sqrt{\text{Re } Z_{Ii}}} \qquad i_i = I_i\sqrt{\text{Re } Z_{Ii}} \tag{1.17}$$

Note that normalized voltages and currents have the same dimension, which is $\sqrt{\text{watt}}$. Hence the relationship between the normalized and the unnormalized parameters can be expressed as

$$[v] = [z][i] \tag{1.18}$$

where

$$[v] = [z_c]^{-1/2}[V] \qquad [i] = [z_c]^{1/2}[I] \tag{1.19}$$

and

$$[z_c] = \text{Re}\begin{bmatrix} Z_{I1} & 0 & 0 & \cdots & 0 \\ 0 & Z_{I2} & 0 & \cdots & 0 \\ \vdots & \vdots & \vdots & \ddots & \vdots \\ 0 & \cdots & \cdots & \cdots & Z_{IN} \end{bmatrix} \tag{1.20}$$

$[z]$ is known as the normalized port impedance matrix, and

$$[y] = [z]^{-1} \tag{1.21}$$

is the corresponding normalized port admittance matrix.

Below we will show how normalized voltage and current matrices account for the interaction of the network with the system that embeds it.

1.4.3 Scattering Matrix

The scattering matrix concept with respect to positive and real terminating impedances was introduced by Penfield [10]. Kurokawa introduced the concept of power wave variables in 1965 [11] and generalized the concept of Penfield.

Following the method due to Kurokawa [11], let us consider a one-port network as shown in Fig. 1.6.

We define the following variables:

$$a_1 = \frac{V_1 + Z_{I1} I_1}{2\sqrt{\text{Re}\, Z_{I1}}} \tag{1.22a}$$

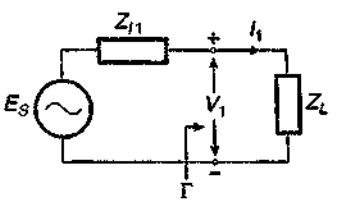

Figure 1.6 One-port network.

$$b_1 = \frac{V_1 - Z_{I1}^* I_1}{2\sqrt{\text{Re } Z_{I1}}} \tag{1.22b}$$

where the asterisk denotes the complex conjugate.

Solving Eqs. (1.22a) and (1.22b), we obtain

$$V_1 = \frac{Z_{I1}^* a_1 + Z_{I1} b_1}{\sqrt{\text{Re } Z_{I1}}} \tag{1.23a}$$

$$I_1 = \frac{a_1 - b_1}{\sqrt{\text{Re } Z_{I1}}} \tag{1.23b}$$

Now, what are the parameters a_1 and b_1?

From Fig. 1.6

$$V_1 = E_s - Z_{I1} I_1 \tag{1.24}$$

Combining Eqs. (1.22a) and (1.24) and subsequently multiplying a_1 by its complex conjugate, we obtain

$$|a_1|^2 = \frac{|E_S|^2}{4 \text{ Re } Z_{I1}} = P_{S,\max} \tag{1.25}$$

The right-hand side of Eq. (1.25) is easily recognized as the maximum power available from the source. Therefore, we can say that $|a_1|^2$ is the incident power from the source into the load Z_L. Using Eqs. (1.22a) and (1.22b), it can be shown that

$$|a_1|^2 - |b_1|^2 = \text{Re}\{V_1 I_1^*\} \tag{1.26}$$

The right-hand side of Eq. (1.26) is the total real power absorbed by the load. Therefore, we can come to the conclusion that $|b_1|^2$ is the power reflected from the load to the source. At this point we define the reflection coefficient

$$\Gamma = \frac{b_1}{a_1} = \frac{V_1 - Z_{I1}^* I_1}{V_1 + Z_{I1} I_1} = \frac{Z_L - Z_{I1}^*}{Z_L + Z_{I1}^*} \tag{1.27}$$

Using Eq. (1.27), the difference between incident and reflected power, or in other words the power absorbed by the load, can be written as

$$P_L = P_{S,\max} - P_{\text{refl}} = |a_1|^2 (1 - \Gamma^2) \tag{1.28}$$

From (1.27), under the matching condition, when $Z_L = Z_{I1}^*$, $\Gamma = 0$.

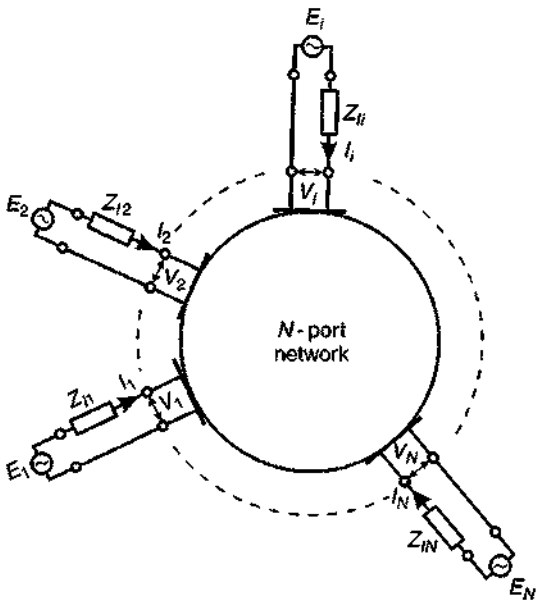

Figure 1.7 Multiport network.

Let us consider the multiport network shown in Fig. 1.7. The scattering matrix of a multiport network can be defined by the equation

$$[b] = [S][a] \tag{1.29}$$

where $[a]$ and $[b]$ are column matrices whose elements are the power wave amplitudes of the incident and reflected waves, respectively, at various ports. If the network has N ports, then $[S]$ is a square matrix of order N.

When the output impedances of the generators connected to the ports of the multiport network become purely real and equal to those of the transmission lines connected to the respective ports, a_i and b_i $(i = 1, 2, 3, \ldots, N)$ become the same as the complex incident and reflected voltages in transmission lines. Then we can write

$$V_i = V_i^+ + V_i^- \tag{1.30a}$$

$$I_i = I_i^+ + I_i^- \tag{1.30b}$$

$$\frac{V_i^+}{I_i^+} = \frac{V_i^-}{I_i^-} = Z_{ii} \tag{1.31}$$

Combining Eqs. (1.30) and (1.22) gives

$$a_i = \frac{V_i^+}{\sqrt{Z_{Ii}}} = \sqrt{Z_{Ii}} I_i^+ \tag{1.32a}$$

$$b_i = \frac{V_i^-}{\sqrt{Z_{Ii}}} = \sqrt{Z_{Ii}} I_i^- \tag{1.32b}$$

and the reflection coefficient is given as

$$\Gamma = \frac{b_i}{a_i} = \frac{Z_L - Z_{Ii}}{Z_L + Z_{Ii}} \tag{1.33}$$

In Eqs. (1.30a)–(1.32), the plus and the minus superscripts denote the ingoing and outgoing parameters, respectively.

The total power absorbed by all the ports is given by the difference between the sum total of the incident and reflected powers of all the ports. Mathematically,

$$P_{\text{total}} = \sum_{k=1}^{N} P_k = \sum_{k=1}^{N} |a_k|^2 - \sum_{k=1}^{N} |b_k|^2 = [a^*]^T[a] - [b^*]^T[b] \tag{1.34}$$

Combining Eqs. (1.29) and (1.34) and the total power absorbed by the network for a lossless condition gives

$$P_{\text{total}} = [a^*]^T[[U] - [S^*]^T[S]][a] = 0 \tag{1.35}$$

where $[U]$ is the unity matrix of order N. From Eq. (1.35) we get

$$[S^*]^T[S] = [U] \tag{1.36}$$

For a reciprocal and symmetrical multiport network, Eq. (1.36) reduces to

$$[S^*][S] = [U] \tag{1.37}$$

which indicates that the scattering matrix of a symmetrical, lossless and reciprocal network is unitary.

Let us write the expanded form of Eq. (1.29):

$$\begin{bmatrix} b_1 \\ b_2 \\ \vdots \\ b_N \end{bmatrix} = \begin{bmatrix} S_{11} & S_{12} & \cdots & S_{1N} \\ S_{21} & S_{22} & \cdots & S_{2N} \\ \vdots & \vdots & \ddots & \vdots \\ S_{N1} & S_{N2} & \cdots & S_{NN} \end{bmatrix} \begin{bmatrix} a_1 \\ a_2 \\ \vdots \\ a_3 \end{bmatrix} \tag{1.38}$$

From Eq. (1.38) it can be seen that, in general,

$$S_{ij} = \frac{b_i}{a_j}\bigg|_{a_k = 0} \qquad k = 1, 2, 3, \ldots, N \qquad k \neq j \tag{1.39}$$

The condition

$$a_k = 0 \tag{1.40}$$

for all k's except $k = j$ is created by perfectly matching all but the jth port. The transmitted signal at the ith port and the incident signal at the jth port are appropriately monitored and S_{ij} is computed using Eq. (1.39). For a detailed description of the procedure the reader is referred to Schiek and Gronefeld [12].

For a given network terminated by a set of real impedances given by $[Z_I]$ in Eq. (1.16) the scattering matrix can be computed by using the following procedure.

- Obtain the port admittance matrix $[Y]$ using nodal analysis and then solving for the node currents.
- Invert the admittance matrix $[Y]$ to obtain the corresponding impedance matrix $[Z]$.
- Normalize $[Z]$ using

$$[z] = [z_c]^{-1/2}[Z][z_c]^{-1/2} \tag{1.41}$$

  where the diagonal matrix $[z_c]$ is obtained from Eq. (1.20).
- Obtain the matrix $[S]$ from

$$[S] = [[z] - [U]][[z] + [U]]^{-1} \tag{1.42}$$

Solving (1.42) gives

$$[z] = [[U] - [S]]^{-1}[[U] + [S]] \tag{1.43}$$

For a reciprocal network, all the matrices associated with the network are symmetrical matrices, which means

$$[Z] = [Z]^T \qquad [S] = [S]^T \qquad \text{etc.} \tag{1.44}$$

1.4.4 Transformation of Scattering Matrix Due to Shift in Reference Planes

Consider Fig. 1.8. The unprimed reference planes $t_j : j = 1, 2, \ldots, N$ are the original reference planes with respect to which the scattering matrix $[S]$ of the N-port network is defined. Now, let us assume that the reference planes are moved away from the network to their new positions marked by the primed letters $t'_j : j = 1, 2, \ldots, N$. The new scattering matrix of the network is given by

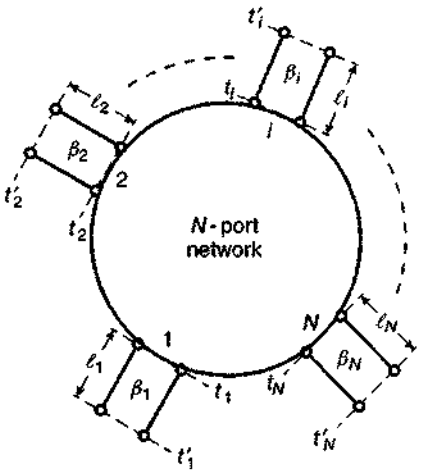

Figure 1.8 Multiport network

$$[S'] = [L][S][L] \tag{1.45}$$

where the matrix

$$[L] = \begin{bmatrix} e^{-j\beta_1 l_1} & \cdots & \cdots & 0 \\ & e^{-j\beta_2 l_2} & \cdots & 0 \\ \vdots & \vdots & \ddots & \vdots \\ 0 & 0 & \cdots & e^{-j\beta_N l_N} \end{bmatrix} \tag{1.46}$$

where β_k is the propagation constant of the wave at the kth port.

All the elements of the scattering matrix of a passive, lossless and reciprocal network cannot be chosen independently. Let us assume that Fig. 1.9 represents one such two-port network whose scattering matrix is given by

$$[S] = \begin{bmatrix} S_{11} & S_{12} \\ S_{21} & S_{22} \end{bmatrix} \tag{1.47}$$

From reciprocity, $[S]$ must be symmetrical. Therefore,

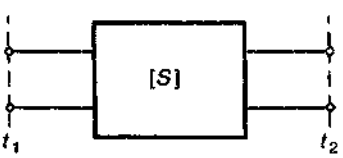

Figure 1.9 Two-port network.

$$[S] = \begin{bmatrix} S_{11} & S_{12} \\ S_{12} & S_{11} \end{bmatrix} = \begin{bmatrix} |S_{11}|e^{j\theta_{11}} & |S_{12}|e^{j\theta_{12}} \\ |S_{12}|e^{j\theta_{12}} & |S_{11}|e^{j\theta_{11}} \end{bmatrix} \tag{1.48}$$

Combining Eqs. (1.37) and (1.48) gives

$$|S_{11}|^2 + |S_{12}|^2 = 1 \tag{1.49}$$

$$\theta_{11} = \theta_{12} \pm \tfrac{1}{2}\pi \tag{1.50}$$

This means that if S_{11} is known in complex form, S_{12} can be obtained from Eqs. (1.49) and (1.50). Equation (1.49) represents conservation of power in a lossless two-port network.

For a lossless nonreciprocal network, the above relations become

$$|S_{11}|^2 + |S_{21}|^2 = |S_{22}|^2 + |S_{12}|^2 = 1 \tag{1.51}$$

$$S_{11}^* S_{12} + S_{21}^* S_{22} = 0 \tag{1.52}$$

$$\theta_{11} + \theta_{22} = \theta_{12} + \theta_{21} \mp \tfrac{1}{2}\pi \tag{1.53}$$

where θ_{21} and θ_{22} are the phase angles associated with the elements S_{21} and S_{22}, respectively.

Scattering Matrix of a Lossless Three-Port Network. An application of unitary condition, given by Eq. (1.36), shows that it is impossible to simultaneously match all the ports of a three-port lossless reciprocal network. However, it is possible to match all three ports if the circuit is lossy or nonreciprocal. The examples are a Wilkinson power divider or a three-port circulator.

At this point it is worthwhile to discuss the usefulness of the scattering matrix. The concept of a scattering matrix is more general than admittance and impedance matrices. Many circuits may not possess an admittance or impedance matrix. Typical examples are ideal transformers having nonfinite elements. On the contrary, such transformers have scattering matrices. According to Carlin [13] and Kajfez [14] all passive networks possess scattering matrices.

In microwave engineering power flow is of primary consideration. Therefore, the scattering matrix is extremely useful. Let us consider the network in Fig. 1.10. Let P_a represent the available power from the generator and P_L the

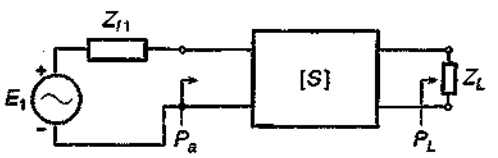

Figure 1.10 Circuit representation of two-port network.

power dissipated in the load R_L. Then it can be shown that the magnitude of the forward transmission coefficient is given by

$$|S_{12}|^2 = \frac{P_L}{P_a} \tag{1.54}$$

Scattering Matrix and the Concept of Insertion Loss. Let us consider the two-port network shown in Fig. 1.11*a*. The transfer coefficient of the network is given by

$$S_{21} = \frac{2V_L}{V_g}\left[\frac{R_g}{R_L}\right]^{1/2} \tag{1.55}$$

Now,

$$|S_{21}|^2 = S_{12}S_{12}^* \tag{1.56}$$

Therefore, from Eqs. (1.55) and (1.56) we obtain

$$|S_{21}|^2 = \frac{|V_L|^2/(2R_L)}{V_g/(8R_g)} = \frac{P_L}{P_a} \tag{1.57}$$

where P_a is the available power from the generator and P_L is the power dissipated in the load R_L. Now, let us consider the network in Fig. 1.11*a*. Suppose we have interposed a two-port network between the reference planes t_1 and t_2, as shown in Fig. 1.11*b*. Let the voltages across the load resistance R_L before and after the interposition of the two-port network be V_L and V_L^p, respectively. Also, let the powers dissipated in R_L before and after the interposition of the two-port network be P_L and P_L^p, respectively. The insertion power ratio of the two-port network is defined as

$$\text{IPL} = \frac{P_L^p}{P_L} \tag{1.58}$$

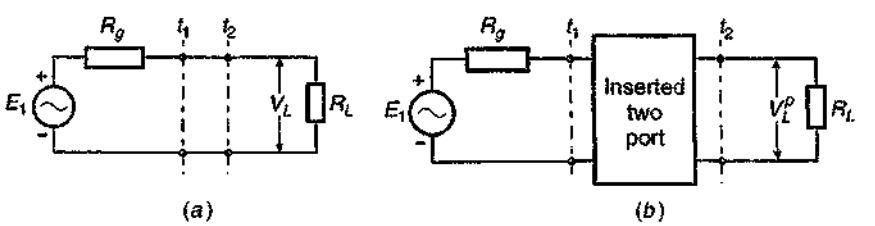

Figure 1.11 (*a*) Two-port network; (*b*) with two-port network inserted.

Analyzing the circuit in Fig. 1.11*b*, we obtain

$$\frac{P_L^p}{P_L} = \frac{|V_g|^2}{|V_L|^2} \frac{R_L^2}{(R_g + R_L)^2} \tag{1.59}$$

Combining Eqs. (1.57) and (1.59) gives

$$\frac{P_L^p}{P_L} = \frac{4R_L R_g}{(R_g + R_L)^2} \frac{1}{|S_{21}|^2} \tag{1.60}$$

Under a perfectly matched condition

$$\frac{P_L^p}{P_L} = \frac{1}{|S_{12}|^2} \tag{1.61}$$

Equation (1.61) is a very useful relationship in network synthesis.

1.4.5 Chain Matrix (*ABCD*) Representation

The chain, or *ABCD*, matrix is particularly useful in cascading or chain connecting microwave networks. The networks may be purely two-port ones or may have multiports. For a single isolated network, the *ABCD* matrix relates the output voltages and currents to the input voltages and currents. Let us consider the multiport network shown in Fig. 1.12. The input voltages and currents are $V_1, \ldots, V_N$ and $I_1, \ldots, I_N$. The output voltages and currents are $V_{N+1}, \ldots, V_{2N}$ and $I_{N+1}, \ldots, I_{2N}$, respectively. The input and the output parameters are related using the following matrix equation:

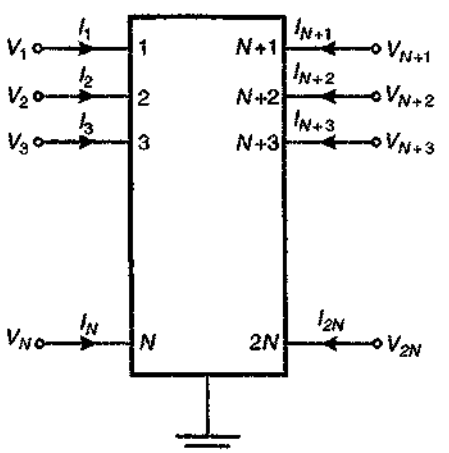

Figure 1.12 Multiport network.

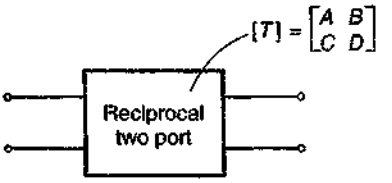

Figure 1.13 Reciprocal two-port network.

$$\begin{bmatrix} V_1 \\ V_2 \\ \vdots \\ V_N \\ I_1 \\ I_2 \\ \vdots \\ I_N \end{bmatrix} = \begin{bmatrix} [A] & [B] \\ [C] & [D] \end{bmatrix} \begin{bmatrix} V_{N+1} \\ V_{N+2} \\ \vdots \\ V_{2N} \\ I_{N+1} \\ I_{N+2} \\ \vdots \\ I_{2N} \end{bmatrix} \tag{1.62}$$

where $[A]$, $[B]$, $[C]$, and $[D]$ are $N \times N$ square matrices. For a two-port network, Eq. (1.62) reduces to

$$\begin{bmatrix} V_1 \\ I_1 \end{bmatrix} = \begin{bmatrix} A & B \\ C & D \end{bmatrix} \begin{bmatrix} V_2 \\ I_2 \end{bmatrix} \tag{1.63}$$

For a reciprocal two-port network, shown in Fig. 1.13, it can be shown that

$$AD - BC = 1 \tag{1.64}$$

or in general,

$$[A][D] - [B][C] = [U] \tag{1.65}$$

where $[U]$ is the identity matrix of order N.

As mentioned above, the $ABCD$ matrix is very useful in obtaining the overall response of a chain connection of a number of two-port networks. Let us consider the chain connection of two two-port networks, as shown in Fig. 1.14.

Let the $ABCD$ matrices of the individual networks be $[T_1]$ and $[T_2]$. Then it can be very easily shown that the $ABCD$ matrix of the cascaded network is given by

$$[T] = [T_1][T_2] \tag{1.66}$$

Equation (1.66) can be generalized for the cascade of more than two networks using the same principle.

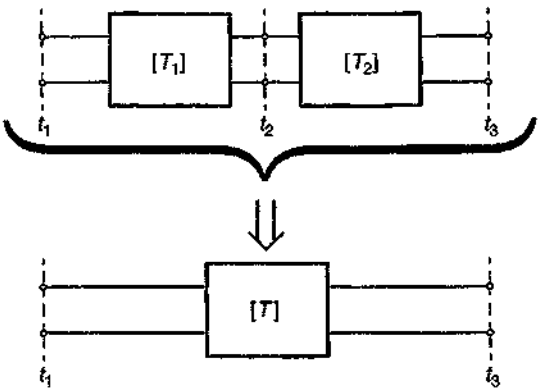

Figure 1.14 Two-port networks in tandem.

Use of ABCD Matrix in Computing Network Properties. In the previous section we have shown that a chain of cascaded two-port networks can be reduced to an equivalent two-port network by finding the overall *ABCD* matrix. Let such an equivalent two-port network be fed at the input port by a voltage source of output impedance Z_g and terminated at the output port by a load Z_L, as shown in Fig. 1.15.

Using Eq. (1.63) and the relationship

$$V_2 = Z_L I_2 \tag{1.67}$$

it can be shown that the input impedance of the network is given by

$$Z_{\text{in}} = \frac{Z_L A + B}{Z_L C + D} \tag{1.68}$$

and the output impedance is

$$Z_{\text{out}} = \frac{Z_g D + C}{Z_g B + A} \tag{1.69}$$

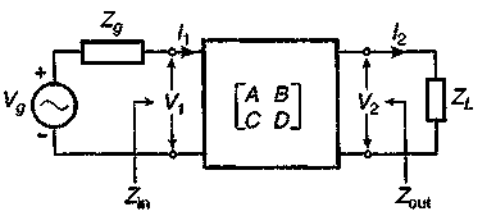

Figure 1.15 Two-port network *ABCD* matrix analysis.

The reflection coefficients looking into the input and the output are given by

$$\Gamma_{\text{in}} = \frac{Z_{\text{in}} - Z_g}{Z_{\text{in}} + Z_g} \tag{1.70}$$

and

$$\Gamma_{\text{out}} = \frac{Z_{\text{out}} - Z_L}{Z_{\text{out}} + Z_L} \tag{1.71}$$

respectively. The voltage gain is given by

$$A_v = \frac{V_L}{V_g} = \frac{V_2}{V_g} = \frac{Z_L}{Z_L A + B + Z_L Z_g C + Z_g D} \tag{1.72}$$

The power is given by

$$G = \frac{P_L}{P_1} = \frac{\text{Re } Z_{\text{in}}}{\text{Re } Z_L} \left| \frac{Z_L}{Z_L A + B} \right|^2 \tag{1.73}$$

where

$$P_1 = V_1 I_1 \tag{1.74}$$

is power delivered to the input port of the network and

$$P_L = V_L I_2 \tag{1.75}$$

is the power delivered to the load. The transducer power gain is given by

$$G_T = \frac{P_L}{P_{AG}} = 4 \frac{\text{Re } Z_g}{\text{Re } Z_L} \left| \frac{Z_L}{Z_L A + B + Z_L Z_g C + Z_g D} \right|^2 \tag{1.76}$$

where P_{AG} is available power from the source.

Normalized ABCD Matrix. Using the normalized voltage and current definitions in Eq. (1.17), we can define the normalized $ABCD$ matrix as follows [14]. Suppose the multiport network in Fig. 1.12 is terminated by a set of impedances Z_{li} $(i = 1, 2, \ldots, 2N)$. Then we can define a set of normalized voltages and currents v_i and i_i respectively $(i = 1, 2, \ldots, 2N)$ according to Eq. (1.17). These normalized voltages and currents can be related using the normalized $ABCD$ matrix as follows:

$$\begin{bmatrix} v_1 \\ v_2 \\ \vdots \\ v_N \\ i_1 \\ i_2 \\ \vdots \\ i_N \end{bmatrix} = \begin{bmatrix} [A_n] & [B_n] \\ [C_n] & [D_n] \end{bmatrix} \begin{bmatrix} v_{N+1} \\ v_{N+2} \\ \vdots \\ v_{2N} \\ i_{N+1} \\ i_{N+2} \\ \vdots \\ i_{2N} \end{bmatrix} \tag{1.77}$$

where $[A_n]$, $[B_n]$, $[C_n]$, and $[D_n]$ are $N \times N$ square matrices. For a two-port network, Eq. (1.77) reduces to

$$\begin{bmatrix} v_1 \\ i_1 \end{bmatrix} = \begin{bmatrix} A_n & B_n \\ C_n & D_n \end{bmatrix} \begin{bmatrix} v_2 \\ i_2 \end{bmatrix} \tag{1.78}$$

The unnormalized and the normalized *ABCD* matrices are related through

$$\begin{bmatrix} [A] & [B] \\ [C] & [D] \end{bmatrix} = \begin{bmatrix} [Z_{IN}]^{-1/2} & [0] \\ [0] & [Z_{IN}]^{1/2} \end{bmatrix}^{-1} \begin{bmatrix} [A_n] & [B_n] \\ [C_n] & [D_n] \end{bmatrix} \begin{bmatrix} [Z_{I2N}]^{-1/2} & [0] \\ [0] & [Z_{I2N}] \end{bmatrix} \tag{1.79}$$

where $[Z_{IN}]$ is a diagonal matrix of real elements $Z_{I1}, Z_{I2}, \ldots, Z_{IN}$ and $[Z_{I2N}]$ is a diagonal matrix of real elements $Z_{I(N+1)}, Z_{I(N+2)}, \ldots, Z_{I(2N)}$. In case of a simple two-port network, Eq. (1.79) reduces to

$$\begin{bmatrix} A & B \\ C & D \end{bmatrix} = \begin{bmatrix} \dfrac{1}{\sqrt{Z_{I1}}} & [0] \\ [0] & \sqrt{Z_{I1}} \end{bmatrix}^{-1} \begin{bmatrix} A_n & B_n \\ C_n & D_n \end{bmatrix} \begin{bmatrix} \dfrac{1}{\sqrt{Z_{I2}}} & [0] \\ [0] & \sqrt{Z_{I2}} \end{bmatrix} \tag{1.80}$$

Obviously the normalized *ABCD* matrix takes into consideration the effects of the impedances terminating the ports of a network. It can be shown that the scattering matrix of a two-port network is related to its normalized *ABCD* matrix via

$$[S] = \begin{bmatrix} A_n + B_n - C_n - D_n & 2(A_nD_n - C_nB_n) \\ 2 & D_n + B_n - A_n - C_n \end{bmatrix} \tag{1.81}$$

REFERENCES

1. Bhartia, P., and I. J. Bahl, *Millimeter Wave Engineering and Applications*, Wiley, New York, 1984.

2. Barrett, R. M., "Microwave Printed Circuits—the Early Years," *IEEE Trans. Microwave Theory Tech.*, Vol. MTT-32, Sept. 1984, pp. 983–990.
3. Barrett, R. M., and M. H. Barnes, "Microwave Printed Circuits," paper presented at the IRE National Conference on Airborne Electronics, Dayton, OH, May 23–25, 1951.
4. Sanders Associates, *Handbook of Tri-Plate Microwave Components*, Sanders Associates, Nashua, NH, 1956.
5. Greig, D. D., and H. F. Engelmann, "Microstrip—a New Transmission Technique for the Kilomegacycle L Range," *IRE Proc.*, Vol 40, Dec. 1952, pp. 1644–1650.
6. King, D. D., "Properties of Dielectric Image Lines," *IRE Trans. Microwave Theory Tech.*, Vol. MTT-3, Mar. 1955, pp. 75–78.
7. Howe, H., "Microwave Integrated Circuits—an Historical Perspective," *IEEE Trans. Microwave Theory Tech.*, Vol. MTT-32, Sept. 1984, pp. 991–996.
8. Mcquiddy, Jr. D. N., J. W. Wassel, J. B. Lagrange, and W. R. Wisseman, "Monolithic Microwave Integrated Circuits: An Historical Perspective," *IEEE Trans. Microwave Theory Tech.*, Vol. MTT-32, Sept. 1984, pp. 997–1008.
9. Collin, R. E., *Foundations for Microwave Engineering*, McGraw-Hill, New York, 1986.
10. Penfield, P., "Noise in Negative Resistance Amplifiers," *IRE Trans. Circuit Theory*, Vol. CT-7, 1960, pp. 160–170.
11. Kurokawa, K., "Power Waves and the Scattering Matrix," *IEEE Trans. Microwave Theory Tech.*, Vol. MTT-13, No. 2, Mar. 1965, pp. 194–202.
12. Schiek, B., and A. Gronefeld, "Standing Wave Meters and Network Analyzers," in *Wiley Encyclopedia of Electrical and Electronics Engineering*, Vol. 20, Wiley, New York, 1999, pp. 403–423.
13. Carlin, H. J., and A. B. Giordano, *Network Theory*, Prentice-Hall, Englewood Cliffs, NJ, 1964.
14. Kajfez, D., *Notes on Microwave Circuits*, Vol. 1, Kajfez Consulting, Oxford, MS, 1986.